Catalysis Today 149 (2010) 76–81

Contents lists available at ScienceDirect

Catalysis Today

journal homepage: www.elsevier.com/locate/cattod

Preparation and properties of nickel preimpregnated CYCTS supports for hydrotreating coker gas oil

Qiang Wei, Yasong Zhou *, Shichang Wen, Chunming Xu

State Key Laboratory of Heavy Oil Processing, China University of Petroleum, Beijing 102249, PR China

ARTICLE INFO

Article history:
Available online 3 July 2009

Keywords:
Ni preimpregnation
Coker gas oil (CGO)
Hydrotreating
Catalyst
Preparation

ABSTRACT

The citric treated Y zeolite composite titania–silica (CYCTS) supports and nickel (Ni) preimpregnated CYCTS supports (NiC*m*, *m* is the Ni content by weight) were prepared by sol–gel combined with CO_2 supercritical drying method. Effects of the Ni concentration on the structure, physical and chemical properties were examined using BET, H_2-TPR, XRD, and UV–vis DRS. Hydrotreating catalysts were prepared with CYCTS or NiC*m* as supports and Ni–tungsten (W) as metal components. The hydrotreating performances of the catalysts were examined with Liaohe coker gas oil (CGO) as feedstock. The results indicated that the Ni preimpregnated supports had suitable mesoporous structure and surface area, and the TiO_2 particles size become smaller. At the same time, the Ni preimpregnation method could promote the formation of highly active nickel species in octahedral sites and improved the dispersivity of WO_3. The hydrotreating performances of the Ni–W catalysts using the NiC*m* supports for Liaohe CGO had been remarkably promoted, especially the hydrodenitrogenation (HDN) performance.

1. Introduction

In recent years, the production of heavy oil increased and caused the properties of crude oil more and more inferior [1,2]. The general residue processing method such as fluid catalytic cracking (FCC) is not suitable for the residue of low quality. However, coking is widely used to process this kind of raw materials [3]. Whereas, coker gas oil (CGO) contains large amount of heteroatom such as sulphur (S), nitrogen (N) and so on [4,5]. Therefore, hydrotreating that removes heteroatom from these feedstocks is of great importance for upgrading the undesirable feedstock to valuable products [6,7]. By this way, S and N concentrations in CGO are reduced and therefore their poisoning effects on cracking catalysts are lessened; poly-aromatics are partly saturated, the crackability of the feedstock can be improved, and coke deposition is reduced; light oil yields are increased and their quality can be greatly improved.

The improvement of hydrotreating performance requires the active metal to be dispersed evenly on the surface of the support in order to generate more active phase [6]. At present, the active metal dispersity, disperse stability and generative capacity of highly active phase of conventional hydrotreating catalyst are not high enough, so the hydrotreating performance is not as ideal. Ni preimpregnation support is a kind of new catalytic materials prepared by the method of sol–gel [8–17]. This kind of supported catalyst featured with larger individual layer disperse amount of active metal than conventional catalysts. Stronger interact can take place between NiO and the support, then the NiO can be inhibited to generate the formation of micro-crystalline, so the NiO has better dispersibility on the surface of the support. Also, during the calcination period of catalyst preparation, the Ni preimpregnation method can inhibit the gathering of NiO and provide more active reaction cavity. Moreover, the catalyst contains higher thermal stability.

Titanium–silica mesoporous mixed oxides, in which titanium is substituted into a silicate framework and the interaction between titania and silica can produce new active sites [18], is an important material that is used as a support for catalysts [19]. The Ni preimpregnated catalysts of TiO_2–SiO_2 as support for CO_2/CH_4 reforming has been reported. However, the acidity of composite titania–silica (CTS) is not strong enough for heavy oil hydrotreating. Herein, Y zeolite is selected to adjust the acidity and pore structure of CTS. And Ni preimpregnated catalysts were prepared for coker gas oil (CGO) hydrotreating. This paper presents a sol–gel method to prepare Ni containing catalyst; the catalysts characterized higher NiO dispersibility and better hydrotreating performance.

2. Experimental

2.1. Preparation of support

2.1.1. CYCTS preparation

The preparation method of CYCTS is the same as that shown in Ref. [20]. HY zeolite powder was dispersed into 0.05 mol/L citric

* Corresponding author. Tel.: +86 10 89733501; fax: +86 10 69724721.
E-mail address: zhys01@cup.edu.cn (Y. Zhou).

0920-5861/$ – see front matter © 2009 Elsevier B.V. All rights reserved.
doi:10.1016/j.cattod.2009.05.009

acid solution and placed quietly at 35 °C for 1 h, and then filtered and washed with deionized water for three times, and finally dried at 120 °C for 3 h. As a result, the CY was obtained. The sol–gel and in situ growth methods were used to prepare CYCTS. Solution A was prepared by dissolving desired amounts of tetrabutoxytitanium (TBOT) and tetraethoxysilane (TEOS) into ethanol separately and then mixing the resulting solutions homogeneously. CY zeolite powders dispersed into solution A by homogeneously stirring. Solution B was obtained by mixing desired amounts of water, acetic acid and ethanol. Under strong stirring, solution B was dropwise added to solution A. After being stirred for 15 min, the sol obtained was aged at room temperature for 24 h to form titania–silica gel, and then the gel was dried by supercritical CO_2 fluid drying at 40 °C and 13 MPa for 3 h and white particles were obtained. After 3 h of calcination at 500 °C in air, the particles of 20–40 meshes in size named as CYCTS were selected as catalyst support.

2.1.2. NiCm preparation

Desirable amount of nickel nitrate was dissolved into solution A and using the preparation procedure as described above. The post-treatment methods of the resulting powders are identical to those used for CYCTS and NiC*m* obtained, where *m* is the concentration of NiO by weight in the support.

2.2. Catalysts preparation and hydrotreating performance of catalysts

First, the supports were impregnated with nickel nitrate aqueous solutions by the equal volume impregnation method at room temperature for 4 h, dried at 120 °C for 3 h and calcined at 500 °C for 3 h. Then, the supports loaded with Ni were impregnated with an ammonium para-tungstate aqueous solution at room temperature for 4 h, dried at 120 °C for 3 h and calcined for 3 h at 500 °C to obtain NiW hydrotreating catalysts, named NiW/NiC*m*. The total concentration of NiO in the catalyst was 5.2% and that of WO_3 was 24%.

The hydrotreating performance of the catalyst was evaluated on a JQ-III hydroprocessing unit, and a commercial CGO sample was chosen as feedstock. The concentrations of S and N in the CGO are 2402 $\mu g\ g^{-1}$ and 4000 $\mu g\ g^{-1}$, respectively. The catalyst loading was 3 ml. The reaction conditions were 380 °C, 6.0 MPa, 1.0 h^{-1} liquid hour space velocity (LHSV), and volumetric ratio of hydrogen to oil is 1000. The catalyst was presulfided with the conditions as follows: the presulfidation solution 2% CS_2/cyclohexane, 300 °C, 4.0 MPa, 6.0 h^{-1}, and 4 h.

2.3. Characterization of supports and catalysts

The specific surface area, pore volume and pore diameter of the supports and the corresponding catalysts were measured on a Micromeritics ASAP-2400 instrument by BET method. Prior to measurement, the samples were degassed under the conditions of 1.6 Pa and 200 °C for 4 h.

The Brönsted (B) and Lewis (L) acidity of the samples were analyzed on a MAGANA 560 FT-IR instrument by pyridine adsorption method. After the samples being purified at 350 °C for 2 h and cooled down to room temperature, pyridine adsorption was performed. The pyridine was desorbed by temperature programming desorption (TPD), and the data were recorded at 200 °C and 350 °C, respectively. The data of 200 °C was the total acidity and the data of 350 °C was the strong acidity. The wavelength of 1450 cm^{-1} and 1540 cm^{-1} was the adsorption site of L acidity sites and B acidity sites, respectively.

The X-ray diffraction (XRD) patterns of the supports were obtained on a DMAX-2400 polycrystalline powder diffraction instrument and the wavelength of the light-source was 1.54 nm. The working voltage and electric current of the target X-ray tube were 40.0 kV and 100.0 mA, respectively.

UV–vis DRS was performed using a UV-4100 UV spectrometer from Hitachi Corporation and the scanned scope of 200–900 nm and scanning frequency of 120 nm/min.

H_2-TPR was carried out on a TP-5000 multifunction adsorption instrument. The catalyst was treated in air at 500 °C for 1 h, after the sample was cooled to 120 °C, then the samples was treated with H_2/Ar, and the temperature was raised to 1000 °C at 10 °C/min. The signal reflected the concentration of H_2 in H_2/Ar variation was recorded by a mass spectrograph.

The concentrations of S and N in the CGO were determined on an ANTEK 7000 N/S analyzer by the method of ultraviolet florescent spectroscopy.

Table 1
BET properties of NiC*m* supports.

Samples	S_{BET} ($m^2\ g^{-1}$)	V_P (ml g^{-1})	D_P (nm)
CYCTS	280	0.80	11.4
NiC1.0	321	0.72	9.0
NiC2.0	332	0.71	8.5
NiC3.0	296	0.63	8.4
NiC4.0	292	0.55	6.8

S_{BET}, BET specific surface area; V_P, pore volume; D_P, pore diameter.

3. Results and discussion

3.1. Pore characterization of NiCm

Table 1 shows the specific surface area and pore volume of NiC*m*. It can be found that the surface area of NiC*m* support is higher than that of CYCTS. With the Ni concentration increasing, the pore volume and pore diameter of the support decreased, especially NiC4.0. Some researchers [21] reported that different kinds of hydroxyl (–OH) existed on the surface of TiO_2–SiO_2 mixed oxides, the –OH and Ni^{2+} from the added NiO combined into chemical compounds. When the amount of NiO reached the critical concentration, the NiO merged into the cage structure of CYCTS, so the surface area, pore volume and pore diameter decreased.

3.2. Crystalline structure of NiCm and NiW/NiCm

Fig. 1 shows the XRD patterns of NiC*m*, it can be found that there is no feature peaks of NiO appeared when the CYCTS is preimpregnated with Ni, this shows us that the NiO disperses much evenly and the formation of NiO is micro-crystalline, even

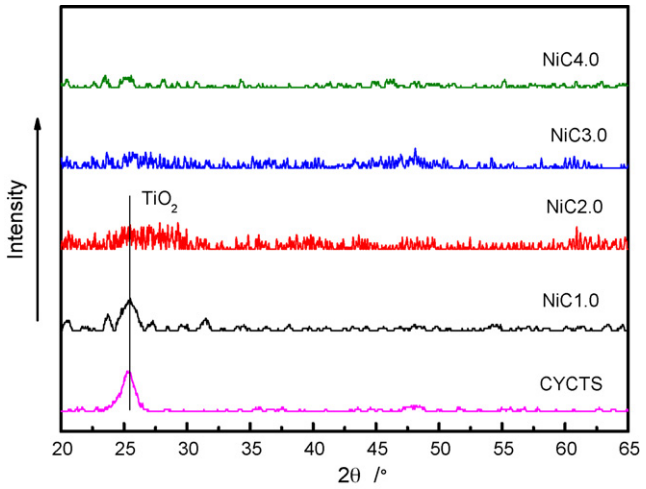

Fig. 1. XRD profiles of NiC*m* supports.

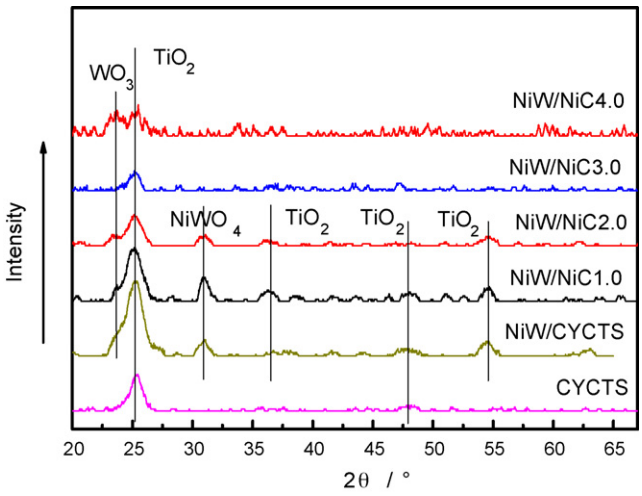

Fig. 2. XRD profiles of NiW/NiC*m* catalysts.

some NiO is emerged into the cage structure and combined with SiO_2 or TiO_2, so NiO cannot be detected by X-ray. Also, we could find that the intensity of feature peaks of TiO_2 decrease with the NiO concentration increasing, even disappear when the concentration of NiO is 3% and 4%, this shows us that the addition of Ni species can accelerate the combination of Ti–O–Si bond and formation of TiO_2 with less particles of microcrystal. This favors for the dispersity of active metal on the surface of the support, thereby the HDN performance of the catalyst should be improved.

Fig. 2 is the XRD patterns of NiW/NiC*m*, it can be found that the feature peaks of WO_3 (23.7°) and $NiWO_4$ (31°) appear both in the spectrum of NiW/NiC*m* and NiW/CYCTS, but the peaks of NiO (36.4°, 43.4°). As to peaks of WO_3, the peaks in spectrum of NiW/CYCTS and NiW/NiC1.0 are shoulder peak but in the spectrum of NiW/NiC4.0 is an independent peak, whereas the intensity of the peak in spectrum of NiW/NiC3.0 is the weakest and barely detected. This illustrates that higher concentration of Ni preimpregnated caused the WO_3 particles dispersed not evenly enough. Peaks of $NiWO_4$ can be found in the spectrum of NiW/NiC1.0, NiW/NiC2.0 and NiW/CYCTS, but the peaks of $NiWO_4$ disappeared in the spectrum of NiW/NiC3.0 and NiW/NiC4.0. This shows us that more concentration of Ni preimpregnated caused the $NiWO_4$ phase disperse more evenly. The $NiWO_4$ phase is the precursor of Ni–W–S, which is the chief activity of hydrotreating catalyst. The higher dispersivity of $NiWO_4$ favors for the sulfidation of the catalyst and improved the hydrotreating performances of the catalyst.

3.3. Acidity of NiCm and NiW/NiCm

Table 2 shows the acidity of CYCTS and NiC*m*. As is seen from the table, the Lewis (L) and Brönsted (B) acidity of CYCTS increased when the support was preimpregnated with Ni. This shows us that

Table 2
Acidity properties of NiC*m* supports.

Samples	Weak (A cm^2 g^{-1})			Strong (A cm^2 g^{-1})		
	L	B	L + B	L	B	L + B
CYCTS	10.5	1.3	11.8	1.1	0.5	1.6
NiC1.0	11.5	2.6	14.1	3.2	3.6	6.8
NiC2.0	13.4	2.0	15.4	4.2	2.6	6.8
NiC3.0	16.0	4.6	20.6	3.6	2.0	5.6
NiC4.0	14.5	4.4	18.9	5.5	3.0	8.5

A, luminous flux.

Table 3
Acidity properties of NiW/NiC*m* catalysts.

Samples	Weak (A cm^2 g^{-1})			Strong (A cm^2 g^{-1})		
	L	B	L + B	L	B	L + B
NiW/CYCTS	12.9	0.8	13.7	2.0	0.9	2.9
NiW/NiC1.0	12.2	1.2	16.8	1.8	1.4	3.2
NiW/NiC2.0	15.6	1.2	16.8	3.6	3.1	6.7
NiW/NiC3.0	18.7	2.5	21.2	2.5	1.8	4.3
NiW/NiC4.0	15.8	2.4	18.2	1.4	0.3	1.7

the preimpregnation of Ni can makes the acidity site and distribution of the CYCTS obviously change. This is because Ni^{2+} is a kind of weak L acidity and makes the L acidity of CYCTS increase when it is preimpregnated. Also, the preimpregnation method can improve the formation of Ti–O–Si bond which is the original of B acidity, so the B acidity of NiC*m* is higher than that of CYCTS.

As to the four NiC*m* supports, with the preimpregnated Ni concentration increasing, both the weak L acidity and B acidity amount are increased to the maximum when the Ni concentration is 3.0 and then fell down later. But the number of the acid sites of L acidity and B of NiC3.0 are minimized. The acidity of support is tightly related with the interaction of active metal and support. Based on the theory of metal-support-interaction (MSI) [22], when the acidity of the support is stronger, the interaction force between metal and support is also stronger; and the metal-support-interaction compounds (MSIC) will be more resistant against reduction and sulfidation treating. The hydrogenization activity of MSIC is the highest when the interaction force is weak. Hereby, the more weak acidity exposed to the surface of the support, the higher of the hydrotreating performance of the supported catalyst is.

Table 3 presents the acidity of NiW/CYCTS and NiW/NiC*m*, it can be found that the L acidity and B acidity distribution of NiW/NiC*m* does not changed a lot comparing with that of NiC*m*, the weak L acidity and B acidity amount keeps very high. Comparing with NiC3.0, the weak L acidity of NiW/NiC3.0 increases but weak B acidity, strong B acidity and strong L acidity amount reduces. This is mainly because the NiO and WO_3 impregnated covered part of the acidity sites of the support, but the Ni^{2+} and W^{6+} are weak L acidity, so the weak acidity amount increases. Former researchers [23,24] reported that L acidity favors for hydrogenation. Molecule simulation on basic nitrogen and non-basic nitrogen hydrotreating also shows that the L acidity favors for the non-basic nitrogen hydrotreating [25].

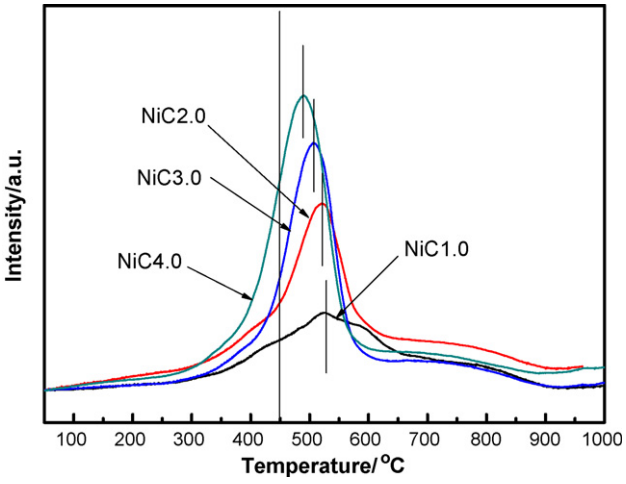

Fig. 3. H_2-TPR profiles of NiC*m* supports.

3.4. H_2-TPR characterization of NiCm and NiW/NiCm

3.4.1. H_2-TPR characterization of NiCm

H_2-TPR is an effective method to characterize the metal-support-interaction. Fig. 3 shows the H_2-TPR profiles of NiC*m*. It can be found that each sample exhibits a feature peak at 500 °C and the feature temperature is higher than the reduction temperature of NiO (about 450 °C). This shows us that the Ni atom takes place some interact with other oxides which make up the support and cause the reduction temperature of NiO increasing. Former researchers [26] reported that Ni atom existed as two formations in the Ni preimpregnated support. That is, some of the Ni atoms emerge into the cavity of oxides and others combine with cage oxides and intensive MSI takes place. The Ni atoms in the cavity have the same properties with the bulk formation Ni atoms but the MSI Ni atoms have higher reduction temperature. The MSI of Ni and support makes the dispersity of Ni atom improved and some of the properties changed. These results are accordant with the results of Fig. 1.

Also, we can find out from Fig. 3 that with the NiO concentration increasing, the integral reduction peak area of NiO increases and reduction temperature decreases, and NiO has the tendency to form the phase of bulk formation. This shows that the MSI of Ni and support is intensive when the Ni loading is low. But with the Ni loading increasing, the MSI of Ni and support is reduced, so the reduction temperature decreases.

3.4.2. H_2-TPR characterization of NiW/NiCm

Fig. 4 presents the H_2-TPR profiles of NiW/CYCTS and NiW/NiC*m*. It can be found that the spectrum of the catalyst contains several temperature intervals no matter what kind of preparation method is used. The interval contains low temperature (L) zone (from 50 °C to 700 °C), middle temperature (M) zone (from 700 °C to 900 °C) and high temperature (H) zone (from 900 °C to 1000 °C higher). As to NiW/NiC1.0, a reduction peak (A) appears from 580 °C to 700 °C, but only a shoulder peak of reduction (B) appears in the profile of NiW/NiC3.0.

Peaks of L zone are the reduction peaks of Ni–W–O (II) and those of M zone are the peaks of Ni–W–O (I). As to NiW/NiC2.0, NiW/NiC3.0 and NiW/NiC4.0, reduction peaks exhibit at H zone, this mainly attributes to the monolayer WO_3 which has the most intensive MSI with support. WO_3 phase is very difficult to be reduced and does not favor for the improvement of hydrotreating performance of the catalyst. As to peak A and B, they reveal the existence of sub-individual layered phase of Ni–W–O species, which are mixture of individual layered Ni–W–O (I) and multi-layered Ni–W–O (II), the reduction temperature of this phase is more close to that of Ni–W–O (II), so are the properties. This shows that the metal oxides of reduction peak A and B reflected have high hydrogenation performance.

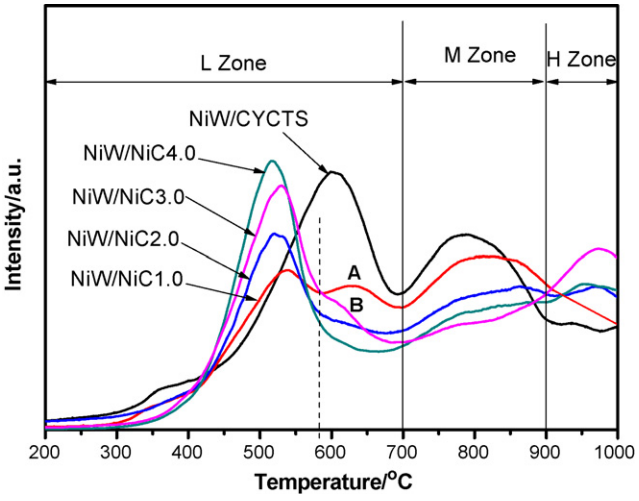

Fig. 4. H_2-TPR profiles of NiW/NiC*m* catalysts.

The profiles of NiW/NiC*m* and NiW/CYCTS differ a lot; this shows that the dispersivity of the active metal on the surface differs much. The reduction peaks of NiW/NiC*m* located in M zone are almost the same as that of NiW/CYCTS, but the reduction temperature of NiW/CYCTS is about 100 °C higher in the L zone than that of NiW/NiC*m*. This shows that the preimpregnated Ni in the support makes the intensity of MSI of active metal and support changed. The decrease of reduction temperature Ni–W–O (II) favors for the reduction and sulphidation of the catalyst, and Ni–W–S (II) specie with higher hydrotreating performance is easier to be generated.

The preimpregnated Ni concentration affects the reduction of catalyst greatly. The reduction temperature, reduction intensity and reduction extent of NiW/NiC*m* differ from each other. This shows that the active metal exposed to the surface of the catalyst is not dispersed evenly enough. In order to describe the amount relation of the species, integration of the L zone, M zone and H zone is carried out. Table 4 lists the integration results of the TPR data.

The amount of Ni–W–O (II) particles is a crucial factor to the hydrotreating performance because Ni–W–O (II) is the precursor of Ni–W–S (II). The species of M zone and H zone are of low activity. As to the four samples prepared by the method of Ni preimpregnation, it can be found that the peak area of L zone of NiC3.0 and NiC4.0 are larger than that of NiC1.0 and NiC2.0. The ratio of integral area of L zone and M zone plus H zone (S_L/S_{M+H}) can also indicate the hydrotreating performance of the catalyst. The calculation results showed that the ratio of S_L/S_{M+H} of NiC3.0 and NiC4.0 was larger than that of NiC1.0 and NiC2.0. This illustrates that the amount of Ni–W–O (II) particles of NiC3.0 and NiC4.0 exposed to the surface of the samples was more than that of NiC1.0 and NiC2.0. Moreover, the reduction temperature of NiC3.0 located in L zone is the lowest, so the Ni–W–O (II) particles are easier to be reduced and sulfide to Ni–W–S (II).

3.5. UV–vis DRS characterization of NiCm

Scheffer et al. [27,28] have done some research on the distribution formation of Ni based on NiO/Al_2O_3 and $NiO–WO_3/Al_2O_3$ by the method of UV–vis. They reported that the Ni atom existed as two coordination status on the surface of the catalysts, one was octahedral (Ni(O)) and the other was tetrahedral (Ni(T)). The absorption peak of tetrahedral Ni atom appeared at 590–640 nm, and the octahedral Ni atom had three broadband absorption peak, they appeared at 302, 467 and 713 nm, respectively. The octahedral Ni species were the active phase of hydrotreating catalyst.

Table 4
Integration of TPR data of NiW/NiC*m* catalysts.

Integration zone		Ni1.0c	Ni2.0c	Ni3.0c	Ni4.0c
L zone (50–700 °C)	Peak location (°C)	537	521	516	530
	Relative peak area	18.3	18.5	19.8	20.1
M zone (700–900 °C)	Peak location (°C)	813	863	900	900
	Relative peak area	14.9	12.2	10.8	10.2
H zone (900–1000 °C)	Peak location (°C)	900	969	959	974
	Relative peak area	5.8	6.5	6.6	7.0
S_L/S_{M+H}	0.88	0.99	1.10	1.11	

S_L/S_{M+H}, ratio of integral area of L zone to M zone plus H zone.

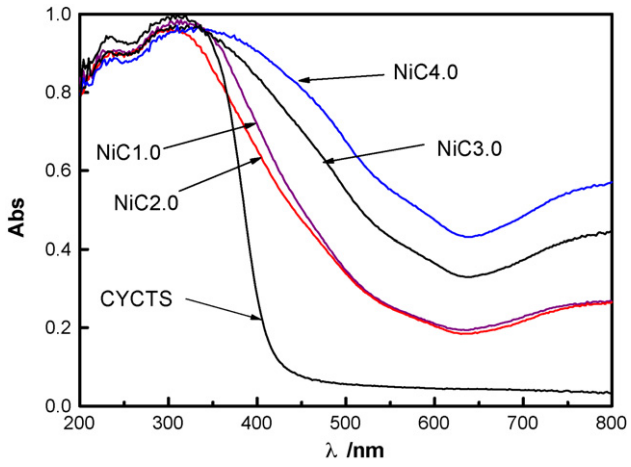

Fig. 5. UV–vis DRS spectrum of NiC*m* supports.

Fig. 5 is the UV–vis DRS spectrum of NiC*m*. It can be found that with the concentration of Ni increasing, the feature peak of sexadentate Ni atom located at 467 nm and 713 nm became more intensive, so the Ni species with high activity increased.

Fig. 6 is the UV–vis DRS spectrum of NiW/NiC*m*. It can be found that the feature peak of sexadentate Ni atom is more intensive than that of NiW/CYCTS. Also, with the preimpregnated Ni concentration increasing, the feature peak of sexadentate Ni atom is more intensive. This denotes that the preimpregnation method favors for the dispersivity of Ni atom on the surface of the catalyst, and accelerates the formation of Ni–W–O (II) with high activation.

3.6. Hydrotreating performance of NiW/NiCm

Table 5 presents the HDN and HDS performance of NiW/NiC*m* and NiW/CYCTS. It can be found that the HDN and HDS conversion of NiW/NiC*m* is higher than that of NiW/CYCTS. This is the results of the improving of the dispersivity of metal (XRD results) and the increasing of the amount of Ni–W–S (II) particles (H_2-TPR results) by the preimpregnation method. So the hydrogenation performance of the catalyst is improved and then the HDS and HDN performance. With the preimpregnated Ni concentration increasing, the HDS and HDN conversions rise up at first and then fall down with the increasing concentration of preimpregnated Ni. The maxima of HDS and HDN conversions are 95.1% and 70.2%, respectively, when the preimpregnated concentration of Ni is 3.0%.

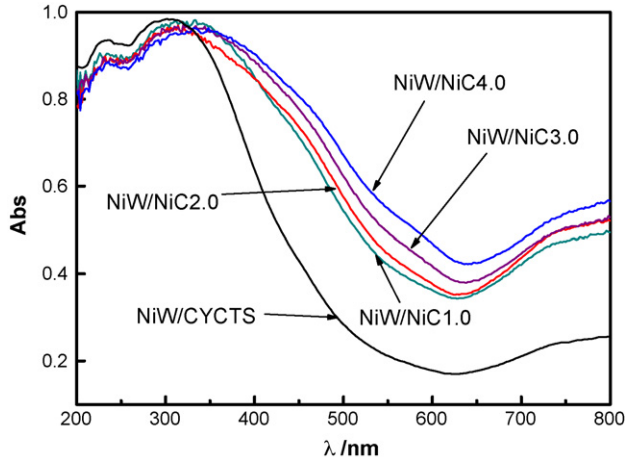

Fig. 6. UV–vis DRS spectrum of NiW/NiC*m* catalysts.

Table 5
HDS and HDN performances of NiW/NiC*m* catalysts.

	Y_{TN} (%)	Y_{BN} (%)	Y_{NBN} (%)	C_{NBN}/C_{BN}	Y_S (%)
NiW/CYCTS	44.4	47.9	42.7	2.3	81.7
Ni1.0c	58.1	55.2	59.4	1.9	89.3
Ni2.0c	64.8	61.2	66.5	1.8	92.5
Ni3.0c	70.2	63.0	73.7	1.5	95.1
Ni4.0c	62.2	62.9	61.2	2.1	93.7

Y_{TN}, conversion of total nitrogen; Y_{BN}, conversion of basic nitrogen; Y_{NBN}, conversion of non-basic nitrogen; Y_S, conversion of sulphur; C_{NBN}/C_{BN}, ratio of concentration of NBN to BN.

The hydrotreating performances are in accordance with the properties of the catalysts. XRD and H_2-TPR results show that active metal on the surface of the catalyst NiW/NiC3.0 disperses the most evenly and the amount of Ni–W–O (II) particles of low reduction temperature is the most. Also, the amount of weak L acidity is the most. These properties are beneficial for the improvement of hydrotreating performances. It can be drawn that the hydrotreating performance of the catalyst can be improved when appropriate amount of Ni is preimpregnated. When too much of Ni is preimpregnated, the surface area and pore volume of the catalyst is reduced because the micro-pores of the catalyst is blocked and causes the hydrotreating performances of the catalyst improve not as much as that of NiW/NiC3.0.

4. Conclusions

(1) The surface area of the support was increased when it was prepared by means of the method of Ni preimpregnation, and the pore volume and pore diameter maintained unchanged. The NiO particles among NiC*m* were micro-crystalline with high dispersivity. The NiO micro-crystalline improved the combination of TiO_2 and SiO_2.
(2) Suitable Ni preimpregnated concentration improved the dispersivity of $NiWO_4$ on the surface of the support and the probability of active metal exposed to the edge of the support.
(3) The acidity of the support was changed by means of the method of Ni preimpregnation, especially the weak L acidity increased. The preimpregnation method was beneficial for the formation of weak MSIC and also the reduction and sulfidation of Ni–W–O (II).
(4) The hydrotreating results showed that the hydrotreating performance of the catalyst was improved by the method of Ni preimpregnation. The HDN conversion increased by 14–26% and HDS increased by 7–14%. The hydrotreating performances of NiW/NiC3.0 are the best among the prepared catalysts, especially the basic nitrogen conversion.

Acknowledgements

The authors acknowledge the financial support from Ministry of Science and Technology of China through the National Basic Research Program (Grant No. 2004CB217807), Natural Science Foundation Committee of China through the Research Program (Grant No. 20876172) and CNPC through the Technology Development Program (Grant Nos. 07-02-05-03-02 and 06A50103).

References

[1] M. Sau, K. Basak, U. Manna, et al. Catal. Today 109 (2005) 112.
[2] G.G. Garifzyanova, G.G. Garifzyanov, Chem. Tech. Fuel Oils 42 (2006) 10.
[3] H. Topsøe, B.S. Clausen, F.E. Massoth, Hydrotreating Catalysis, Springer, Berlin, 1996.
[4] M. Breysse, G. Djega-Mariadassou, S. Pessayre, et al. Catal. Today 84 (2003) 129.
[5] T.C. Ho, Catal. Today 98 (2004) 3.
[6] M. Egorova, R. Prins, J. Catal. 221 (2004) 11.
[7] G. Laredo, J. Delos Reyes, J. Cano, J. Castillo, Appl. Catal. A 207 (2001) 103.
[8] E. Hensen, Y. Meer, J. Veen, et al. Appl. Catal. A: Gen. 322 (2007) 16.

[9] E. Adolfo, Castro Luna, E. Marı′a, Iriarte, Appl. Catal. A: Gen. 343 (2008) 10.
[10] E. Tkalcec, S. Kurajica, J. Schmauch, J. Non-Crystal. Sol. 353 (2007) 2837.
[11] O. Mekasuwandumrong, N. Wongwaranon, J. Panpranot, et al. Mater. Chem. Phys. 111 (2008) 431.
[12] J. Grzechowiak, I. Szyszka, A. Masalska, Catal. Today 137 (2008) 433.
[13] S. Nandya, S. Mallick, P.K. Ghosh, et al. J. Alloy Compd. 453 (2008) 1.
[14] C. Suciu, A.C. Hoffmann, E. Dorolti, et al. Chem. Eng. J. 140 (2008) 586.
[15] S. Zhang, J. Wang, H. Liu, X. Wang, Catal. Commun. 9 (2008) 995.
[16] N. Wongwaranon, O. Mekasuwandumrong, P. Praserthdam, et al. Catal. Today 131 (2008) 553.
[17] M.E. Rivas, J.L.G. Fierro, R. Guil, et al. Catal. Today 133–135 (2008) 367.
[18] X. Gao, I.E. Wachs, Catal. Today 51 (1999) 233.
[19] R.J. Davis, Z. Liu, Chem. Mater. 9 (1997) 2311.
[20] Y. Zhou, Q. Wei, H. Ma, et al. Catal. Today 125 (2007) 211.
[21] Y. Zhu, X. Lin, Y. Ma, et al. J. Mol. Catal. (China) 12 (1998) 417.
[22] M. Zhang, Z. Jin, Z. Zhang, et al. J. Henan Univ. (Natural Science) 35 (2005) 21.
[23] Y. Li, Y. Zhou, Q. Liu, Acta Petrol Sin. (Petroleum Processing Section) 21 (2005) 12.
[24] S. Zhang, Y. Zhou, C. Xu, J. Chem. Indus. Eng. (China) 57 (2006) 770.
[25] M. Sun, A. Nelson, J. Adjaye, J. Mol. Catal. A: Chem. 222 (2004) 243.
[26] Y. Zhu, Z. Wang, Y. Ma, et al. J. Petrol. Chem. Univ. 11 (1998) 19.
[27] B. Scheffer, J. Heijeinga, J. Moulijn, J. Phys. Chem. 91 (1987) 4752.
[28] B. Tang, Q. Jiang, X. He, et al. J. Anal. Sci. 14 (1998) 31.